

Article

Thermal Behavior and Flammability of Epoxy Composites Based on Multi-Walled Carbon Nanotubes and Expanded Graphite: A Comparative Study

Alexander G. Bannov ^{1,*}, Olga B. Nazarenko ² , Evgeny A. Maksimovskii ³, Maxim V. Popov ^{1,4} and Irina S. Berdyugina ¹

¹ Department of Chemistry and Chemical Technology, Novosibirsk State Technical University, 630073 Novosibirsk, Russia; popovmv@ioc.ac.ru (M.V.P.); irina_berdyugina@mail.ru (I.S.B.)

² School of Non-Destructive Testing, Tomsk Polytechnic University, 634050 Tomsk, Russia; obnaz@mail.ru

³ Institute of Inorganic Chemistry, Siberian Branch, Russian Academy of Sciences, 630090 Novosibirsk, Russia; eugene@niic.nsc.ru

⁴ Zelinsky Institute of Organic Chemistry, Russian Academy of Sciences, 119991 Moscow, Russia

* Correspondence: bannov@corp.nstu.ru

Received: 12 September 2020; Accepted: 30 September 2020; Published: 2 October 2020



Abstract: Reduction of flammability and improvement of thermal stability of polymers during heating can be achieved by the introduction of fillers. Epoxy composites filled with different loadings of multi-walled carbon nanotubes (MWCNTs) and expanded graphite (EG) were prepared. The thermal oxidation stability of the prepared samples was investigated under heating in an oxidizing atmosphere using thermal analysis. The hardness was measured using the Shore D hardness test. The flammability of the prepared composites was evaluated by the ignition temperature and time-to-ignition. It was found that there was a rise in temperature corresponding to a 5% weight loss during heating for both epoxy/MWCNT and epoxy/EG composites compared to neat epoxy resin. The Shore D hardness of epoxy/MWCNT composites increased with content growth up to 0.1 wt.% and decreased with further concentration rise. The addition of MWCNTs and EG leads to an increase in the ignition temperature. It has been shown that MWCNTs improve the thermal behavior of epoxy resin in a low temperature region (below ~300 °C) whereas EG shows almost the same thermal behavior above 300 °C. The improvement of thermal properties can be achieved using MWCNTs and EG as fillers.

Keywords: epoxy composites; thermal oxidative degradation; flammability; multi-walled carbon nanotubes; expanded graphite; exfoliated graphite

1. Introduction

Polymers are widely used in industry, science, and our daily life, due to a wide range of properties, including light weight and easy processing, chemical resistance, high strength, electrical insulating properties, etc. [1,2]. Among various types of polymers, epoxy resins are one of the most popular thermosetting polymers. Epoxy resins have excellent chemical and corrosion resistance, high adhesion, good mechanical properties, and low shrinkage [3,4]. The main disadvantage of polymer materials, including epoxy resins, is their high flammability, making them a fire hazard [5,6]. The growth in consumption of polymers has led to an increase in the number of fires and, as a result, damage to property and threat to life. Therefore, the problem of reducing the flammability of polymers and giving them heat-resistant properties is of great importance.

One of the most common and effective ways to achieve enhancement in the properties of polymers, including flame retardant properties and thermal stability, is the incorporation of fillers of an inorganic and organic nature into epoxy resin [7–12]. In recent years, special attention was paid to the use of nanodispersed materials as fillers. In contrast to conventional coarse flame-retardant additives, the effectiveness of the flame-retarding properties of which is achieved at high loading (50 wt.% or more), nanodispersed fillers can contribute to solving the problem of reducing the flammability of polymers at relatively low loading (<5%) [7,13–15]. Generally, the nanodispersed fillers act as barriers against oxygen and combustion gas and produce, during combustion, strong, dense, and crack-free nanocoating surface layers.

Owing to their unique physical properties, carbon nanomaterials, such as carbon nanotubes [16] and nanofibers [17], graphene [18–20], graphene nanoplatelets [21], reduced graphene oxide [22], graphene oxide [23,24], and expanded graphite [25], have attracted great attention in recent years, particularly for the improvement of flame retardancy of epoxy composites [26–34].

A comparison of thermal degradation of epoxy composites and multi-wall carbon nanotubes (MWNTs) was studied in [33]. It was found that the preparation technique has an important role in the formation of thermal behavior characteristics. Jen et al. [35] found the synergetic effect of the ratio of MWCNT and graphene nanoplatelets (9:1 ratio MWCNT:graphene nanoplatelets) on the thermomechanical properties of epoxy composites. Kuan et al. [36] reported the enhancement of flame retardancy of epoxy resin based on functionalized multi-walled carbon nanotubes obtained by the sol-gel technique. It was found that the activation energy of the degradation reaction increased when increasing carbon nanotubes content, and after reaching 7 wt.%, it began to decrease.

Gantayat et al. [37] used the solution-mixing method for preparation of epoxy/expanded graphite composites. They reported an increase in thermal degradation temperature due to the enhanced dispersion of expanded graphite in the epoxy matrix. Asante et al. [38] studied the thermal degradation of epoxy/expandable graphite composites. The weight percentage of EG in the studied epoxy composites was 1, 3 and 5 wt.%. It was found that the time-to-ignition, the critical heat flux, the ignition temperature, the thermal inertia, the smoke yield, and the peak heat release rate decreased with the increasing EG content in the epoxy composites. Despite the presence of a lot of publications devoted to epoxy resin based on multi-walled carbon nanotubes and expanded graphite, there are not enough data on filler concentration effect at a low filler content on thermal behavior and flammability.

The aim of this work is to study the effects of carbon nanofillers, multi-walled carbon nanotubes and expanded graphite (EG), taken in different concentrations, on the thermal oxidative degradation, hardness, and flammability of the epoxy composites.

2. Materials and Methods

2.1. Materials and Sample Preparation

The epoxy resin DER-331 based on Bisphenol A (Dow Chemical, Germany) was used as a polymer matrix. The epoxy resin DER-331 contains 22.4–23.6% epoxy groups; the average molecular weight of the resin is 340 g/mol. Polyethylenepolyamine (PEPA) was used as a curing agent (ZAO Uralkhimplast, Nizhny Tagil, Russia).

The multi-walled carbon nanotubes used in this work were supplied by Shenzhen Nano-Tech Port Co. (MWCNT-4060 grade).

Thermally-expanded graphite was produced from commercial intercalated graphite (EG-350-50 brand, “Khimicheskiesystemy” Co., Russia) using the method of programmable heating [39]. According to this method, expanded graphite was obtained from intercalated graphite by heating it at a rate of 20 °C/min to a temperature of 500 °C.

The epoxy resin was heated to 55 °C from room temperature (heating rate was 10 °C/min), and then the required amount of fillers was added into the epoxy resin using mechanical stirring for 10 min; afterwards, PEPA was added into mixture. The ratio of epoxy resin and PEPA was 6:1 by weight.

The curing of the samples was conducted at room temperature (25 ± 2 °C) for 24 h. The formulations of the studied epoxy composites are given in Table 1. The loading of MWCNTs ranged from 0.01 to 0.5 wt.%, whereas the loading of EG was in the range from 0.5 to 2.5 wt.%, and the upper limit of filler concentration was taken according to its bulk density. It was not possible to obtain high-quality samples of epoxy/MWCNTs with the loading of the latter above 0.5 wt.%.

Table 1. Formulations of epoxy composites (wt.%).

Sample Code	Epoxy Resin	MWCNTs	EG
E0	100	0	0
E/0.01MWCNT	100	0.01	0
E/0.05MWCNT	100	0.05	0
E/0.1MWCNT	100	0.1	0
E/0.5MWCNT	100	0.5	0
E/0.5EG	10	0	0.5
E/1.0EG	100	0	1.0
E/1.5EG	100	0	1.5
E/2.0EG	100	0	2.0
E/2.5EG	100	0	2.5

2.2. Characterization

Transmission electron microscopy (TEM) of carbon nanotubes was carried out using JEM-2010 (JEOL) microscope.

The defectiveness of carbon materials was studied using a T64000 Horiba Jobin Yvon Raman spectrometer ($\lambda = 514$ nm). Each time, before recording the spectra from the samples, a test spectrum from monocrystalline silicon was recorded. This made it possible to calibrate the device both in the position of the frequencies (the frequency of the long-wavelength optical phonon in silicon is well known and equal to 520.6 reciprocal centimeters) and in the intensity of signals. The spectrometer T64000 and argon laser are highly stable and reproducible. The monochromator used standard gratings for the visible range—1200 lines per millimeter. All Raman spectra were excited with a 514.5 nm Ar^+ laser line in the back-scattering geometry. A triple spectrometer T64000 Horiba Jobin Yvon with micro-Raman setup and CCD multi-channel detector cooled by liquid nitrogen was used. To avoid local overheating of the samples, the laser beam was slightly unfocused (diameter of spot was about 10 micrometers, the laser power reaching the sample was about 1 mW). All spectra were measured at room temperature. The spectral resolution was not worse than 1.5 cm^{-1} . Integration time was 10 s, 6 signal accumulations were made at each point.

Morphology of the surface of the samples obtained was investigated with a S-3400N (Hitachi) scanning electron microscope (SEM) without sputtering. Textural characteristics were evaluated using a Nova 1200e analyzer (Quantachrome). The weight distribution of particles was carried out with a Microsizer 201 (VA Instruments) laser analyzer of particles. Investigation of chemical composition of surface of the samples was performed using X-ray photoelectron spectrometer (SPECS Surface Nano Analysis GmbH, Germany). Spectrometer was equipped with the PHOIBOS-150 hemispherical analyzer and the source of X-ray radiation XR-50M with Al/Ag anode. Al $K\alpha$ ($h\nu = 1486.74 \text{ eV}$) monochromized radiation was used.

Thermal behavior at the heating of the prepared epoxy composites from 20 °C to 700 °C was studied using the thermal analyzer STA 449C Jupiter (Netzsch, Germany). The thermogravimetric (TG) analysis and differential scanning calorimetry (DSC) were carried out at the heating rate of 10 °C/min in air (25 sccm). Samples of approximately 5 mg were placed in an Al_2O_3 crucible with a lid. The samples used for thermal analysis were slightly ground to powder in mortar for all the experiments, to obtain a homogeneous powder and provide uniform heating of the sample in a crucible.

The hardness was measured using the Shore D hardness test. The sample was placed under the indenter, and then the pressure was applied, such that the indenter comes into contact with the sample.

The test was conducted according to ASTM D2240 at 25 °C. Ten samples of each filler and its loading were taken for testing.

The flammability of the prepared epoxy composites was studied according to the standard method of experimental determination of the ignition temperature of solid substances and materials was used in accordance with the national standard of Russian Federation GOST 12.1.044-89 (ISO 4589-84) "Occupational safety standards system. Fire and explosion hazard of substances and materials. Nomenclature of indices and methods of their determination". Samples of a cylindrical shape with a diameter of 31.4 mm and a weight of 6 ± 0.1 g were placed inside a furnace chamber and gradually heated from ambient temperature to the ignition temperature. The ignition temperature was determined at a point when a flame ignited on application of a pilot flame. Six tests were conducted for each sample.

3. Results and Discussion

3.1. Characterization of Fillers

MWCNTs have a diameter of 15–40 nm and a length of 3–5 μm (Figure 1a–c). From the images, it can be seen that the MWCNT sample is represented by long nanotubes with a large number of walls and a hollow channel inside. The diameter of the channel was below 10 nm. Additionally, there was some amount of carbon nanofibers with the cup-stacked structure in the sample. According to TEM, the sample also contained catalytic nanoparticles. The particle size distribution of the MWCNT sample is shown in Figure 1d. The data show that the sample consisted of aggregates of carbon nanotubes, with the predominant particle size ranging from 5 to 280 μm . Since it was not possible to determine the particle size of EG using sedimentation analysis, the grain size was determined using sieves. There were the following fractions of the sample of EG (wt.%): above 500 μm —47.4%, 250–500 μm —45.3%, 200–250 μm —4.3%, 100–200 μm —2.5%, below 100 μm —0.5%.

According to data of TG obtained in the oxidative atmosphere, the ash content in the material was 8.37% (Figure 1e). At the same time, the ash content of the EG sample was only 5.14% which corresponds to a relatively lower amount of impurities and a high fraction of carbon in the material.

SEM images of the EG sample are shown in Figure 2b–d. Figure 2a shows the worm-like particles obtained as a result of the rapid heating of intercalated graphite. The structure of graphite was porous. The pores were formed during the release of the gas phase under heating of intercalated graphite and therefore the sample is represented by the strongly-entangled graphite platelets.

Figure 3 shows the Raman spectra of MWCNTs and EG. There are two main peaks in the Raman spectra. The D peak corresponds to defect structure in carbon materials. The G peak corresponds to the ordered graphite structure in the material [40,41]. The positions of the D and G peaks for the MWCNTs were 1345 cm^{-1} (full width at half maximum (FWHM) 50 cm^{-1}) and 1572 cm^{-1} (FWHM 42 cm^{-1}), respectively. Expanded graphite showed the shift of positions towards higher angles, D (1356 cm^{-1} , FWHM 84 cm^{-1}) and G (1584 cm^{-1} , FWHM 20 cm^{-1}), confirming the well-ordered structure of the material, which is closer to graphite. The ratio of intensities $I(\text{D})/I(\text{G})$ makes it possible to estimate the disorder degree of the MWCNTs and EG, and it was 0.84 and 0.1, respectively. The Raman spectrum of MWCNTs shows their relatively high defectiveness closer to the level of defects of carbon nanofibers [42], whereas the expanded graphite has a low intensity of D peak that confirms the high graphitization degree of the material.

Investigation of textural characteristics showed that the MWCNT sample is fully mesoporous with the surface area $128\text{ m}^2/\text{g}$. The average pore diameter and total pore volume were 10.8 nm and $0.346\text{ cm}^3/\text{g}$. The EG sample had a higher porosity compared to the MWCNTs. Its surface area was $593\text{ m}^2/\text{g}$ with the domination of mesopores ($448\text{ m}^2/\text{g}$) and a lower fraction of micropores ($145\text{ m}^2/\text{g}$). The average pore diameter was lower compared to the MWCNTs (4.3 nm) and the total pore volume was also lower ($0.198\text{ cm}^3/\text{g}$).

The role of surface oxygen-containing functional groups is important for the formation of an interface between epoxy resin and fillers; therefore, it is necessary to determine the concentrations of these groups using X-ray photoelectron spectroscopy (XPS). An XPS spectrum of the MWCNT sample was mentioned in [43] (original sample name was iMWCNT). The XPS spectrum of the EG sample is in the Supplementary Materials (Figure S1). Both samples contain C-O, C=O, and O-C=O functional groups. The O/C ratio was 0.1 (EG) and 0.04 (MWCNTs), showing the higher concentration of oxygen on the surface of the expanded graphite sample. However, it can be noted that the concentration of functional groups was relatively low.

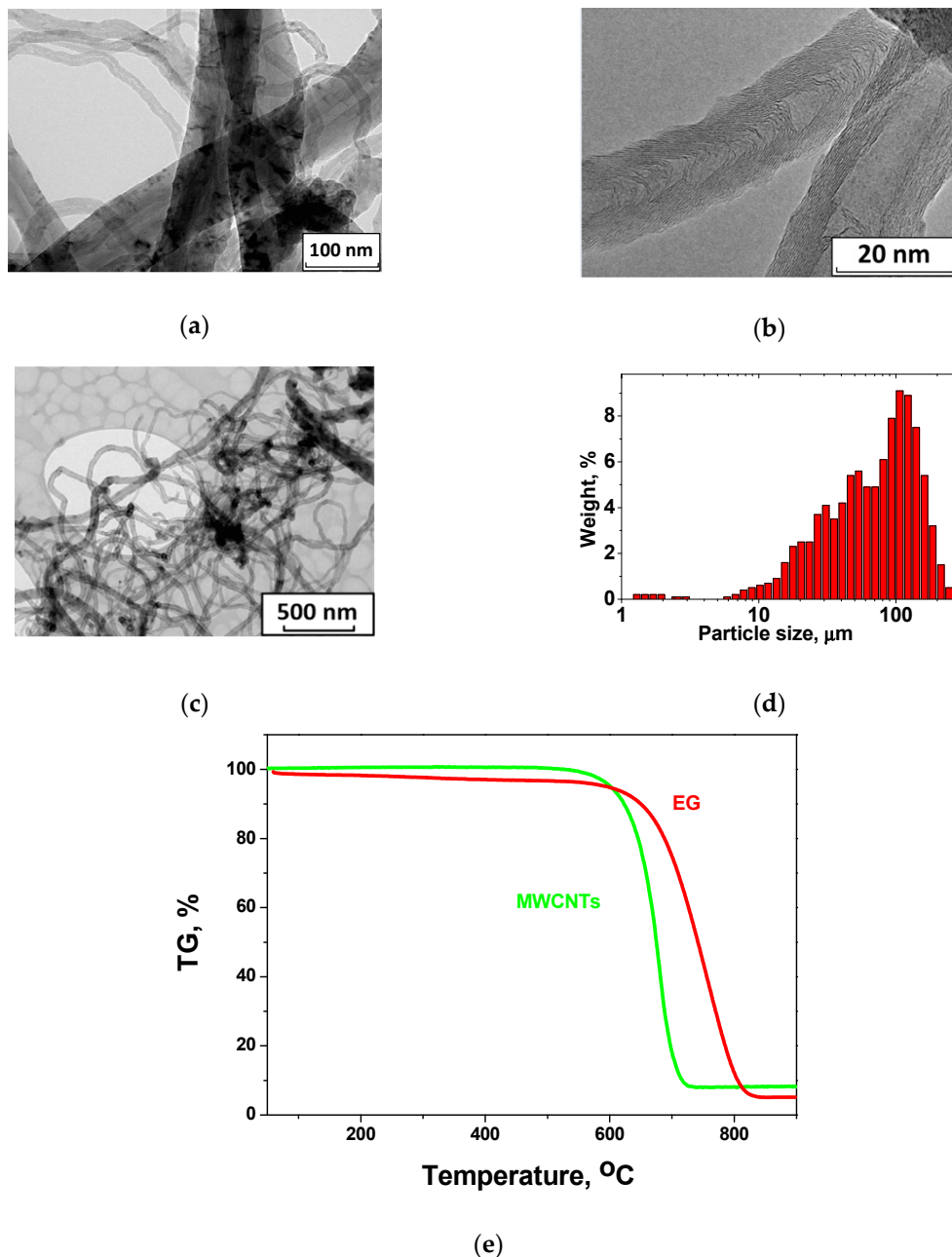


Figure 1. (a–c) Transmission electron microscopy (TEM) images of multi-walled carbon nanotubes (MWCNTs); (d) particle size weight distribution of MWCNTs; (e) thermogravimetric (TG) curves of MWCNTs and expanded graphite (EG).

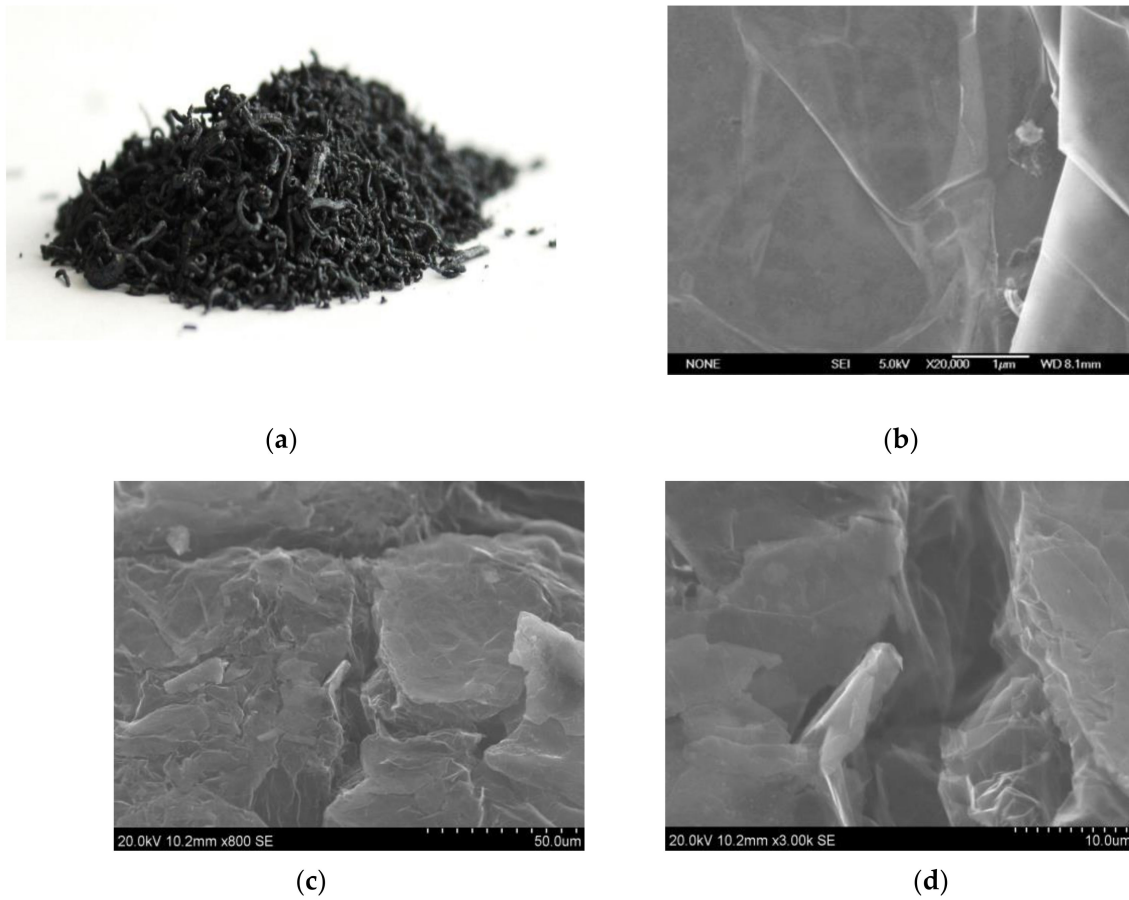


Figure 2. (a) Appearance of EG; (b–d) SEM images of EG.

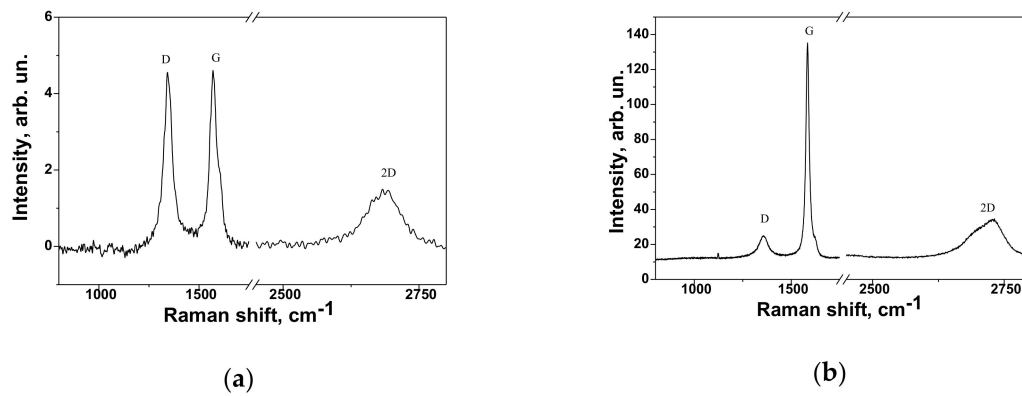


Figure 3. Raman spectra of MWCNTs (a) and EG (b).

3.2. Thermal Oxidation Behavior

Figure 4 shows typical TG and DSC curves of the epoxy composites studied.

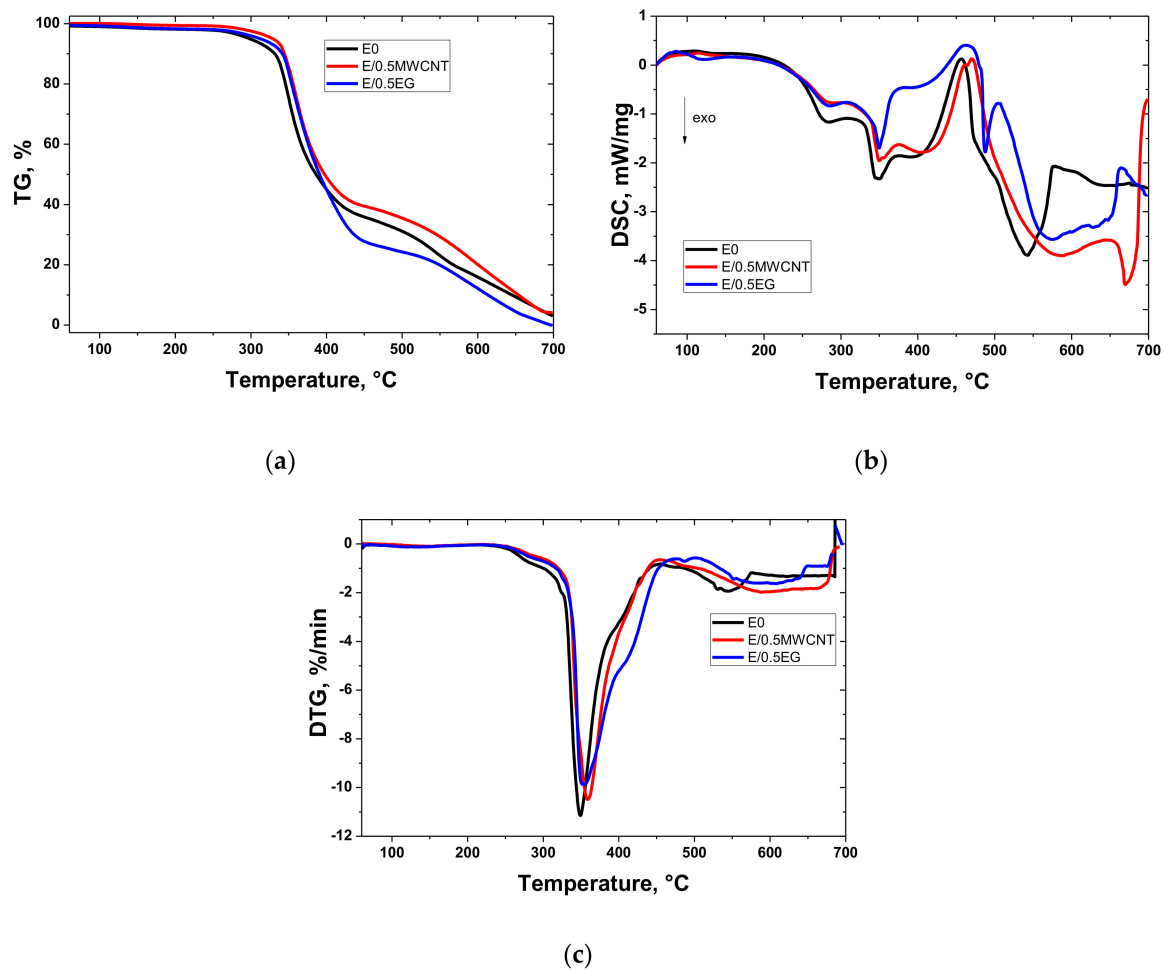


Figure 4. Thermal degradation curves of epoxy composite samples E0, E/0.5MWCNT, E/0.5EG: (a) TG, (b) differential scanning calorimetry (DSC), and (c) derivative thermogravimetry DTG curves.

The thermal degradation process of epoxy resin and epoxy composites when they are heated in an oxidizing environment can be divided into a few steps [44]. The first step is up to ~300 °C. The endothermic peak was observed on DSC curves around 85–120 °C and this process is accompanied by slight weight loss. The second step (~300–500 °C) is caused by the thermal degradation of epoxy resin and the formation of gaseous products as a result of interaction of epoxy resin macromolecules with oxygen. Increasing the temperature above 500 °C leads to the oxidation of the filler and increases its contribution to the degradation process.

The TG results of the neat epoxy polymer E0 and all of the epoxy composites are summarized in Table 2.

The incorporation of MWCNTs into the epoxy matrix led to an improvement in thermal stability. For the epoxy/MWCNTs composites, a sharp rise in temperature of 5% mass loss $T_{5\%}$ was observed from 300 °C for the pure epoxy resin E0 to 319 °C for the epoxy composite filled with 0.1 wt.% of MWCNTs. With a further increase in the content of MWCNTs to 0.5 wt.%, there was a slow increase in $T_{5\%}$ to 326 °C. The values of $T_{5\%}$ were high enough compared to epoxy composites based on expanded graphite and graphene nanoplatelets [45,46], taking into account relatively low concentrations of EG (E/1.0EG) and the increased $T_{5\%}$ (338 °C).

Table 2. Temperatures corresponding to the certain weight loss of epoxy composites during heating.

Sample	$T_{5\%}$	$T_{20\%}$	$T_{50\%}$	$T_{80\%}$
E0	300	352	385	568
E/0.01MWCNT	301	352	389	574
E/0.05MWCNT	312	354	389	582
E/0.1MWCNT	319	352	390	563
E/0.5MWCNT	326	353	396	598
E/0.5EG	316	352	392	548
E/1.0EG	338	356	392	552
E/1.5EG	310	352	395	580
E/2.0EG	315	352	400	682
E/2.5EG	305	350	388	656
MWCNTs	563	600	625	644
EG	595	687	741	785

Notation: $T_{5\%}$, $T_{20\%}$, $T_{50\%}$, $T_{80\%}$ —temperatures (in °C), corresponding to 5%, 20%, 50%, and 80% mass loss of the sample, respectively. The values for fillers were given for comparison.

The values of temperature $T_{20\%}$ for the epoxy/MWCNTs composites were slightly higher or close to that for the pure epoxy resin E0. The temperature of 50% mass loss $T_{50\%}$ slightly increased with increasing the concentration of MWCNTs in the epoxy matrix. The highest temperature $T_{80\%}$ of 598 °C was achieved on the sample E/0.5MWCNT, although for the sample E/0.05MWCNT, a local maximum with $T_{80\%}$ of 582 °C was also observed. This effect can be linked with a high concentration of filler and its ability to absorb the products of oxidative degradation of sample.

It is worth noting that the bulk density of the EG and MWCNTs was 0.018 g/cm³ and 0.065 g/cm³, respectively. This fact indicates that expanded graphite has a significantly higher volume fraction in the composite at the same weight of filler. Of course, the increase in concentration of carbon nanotubes could neutralize this effect; however, taking into account the wetting of the filler and the results of preliminary experiments, it has been shown that the upper limit of concentration of the MWCNTs was 0.5 wt.%.

When adding EG, the value of $T_{5\%}$ increased compared to that of the pure epoxy resin E0, reaching a maximum at a concentration of 0.5 wt.% EG, and decreased with a further increase in concentration. It is interesting that $T_{20\%}$ values of the epoxy/MWCNTs and epoxy/EG composites are almost the same and equal to that of the E0 sample, whereas $T_{50\%}$ is higher in the entire concentration range of MWCNTs and EG compared to the neat epoxy resin. The thermal behavior of epoxy composites within a temperature range of $T_{80\%}$ is determined mainly by the filler. The temperatures $T_{80\%}$ are higher for the samples filled with EG than MWCNTs which is caused by the higher graphitization degree of expanded graphite. The higher disorder degree of MWCNTs compared to EG can be confirmed by the I(D)/I(G) ratio of the Raman spectrum (Figure 3). In [47], it was reported that the expanded graphite did not improve the thermal oxidative behavior of the epoxy/EG composite. On the other hand, our data on $T_{5\%}$ showed that this temperature shifts towards higher temperatures when adding up to 2.5 wt.% EG, whereas in [47], authors used an extremely wide range of concentrations (5–50 wt.%). It is worth noting that the expanded graphite that we used in our study begins to oxidize at 623 °C (Figure S2 in Supplementary Materials), therefore the contribution of filler oxidation in the oxidation of the entire composite can be related to its interaction with the epoxy matrix. Taking into account that the oxygen content is higher for the EG sample, it will form a stronger interaction at the interface.

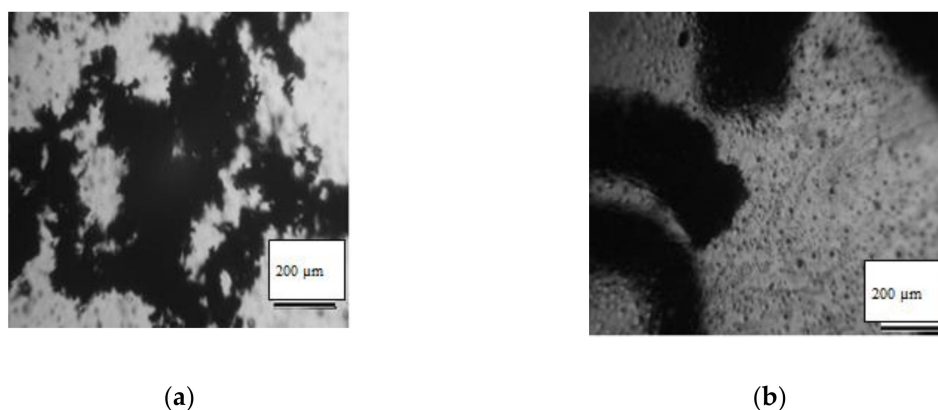
3.3. Hardness

The results of the hardness (Shore D test) are presented in Table 3.

Table 3. Shore D hardness results of epoxy/MWCNTs and epoxy/EG composites.

Sample	Hardness
E0	78 ± 2
E/0.01MWCNT	79 ± 3.2
E/0.05MWCNT	79 ± 1.7
E/0.1MWCNT	81 ± 1.1
E/0.5MWCNT	75 ± 2.3
E/0.5EG	80 ± 1.1
E/1.0EG	76 ± 2.5
E/1.5EG	73 ± 2.2
E/2.0EG	77 ± 1.4
E/2.5EG	78 ± 2.1

The hardness of the neat resin was 78. The addition of MWCNTs slightly increased the hardness. There was no significant increase in the hardness below 0.05 wt.% loading because of relatively low filler concentration. The increase in MWCNT loading above 0.1 wt.% led to a decrease in hardness and it became lower than that of neat resin. This is probably due to the growth of the concentration of air bubbles coming from porous filler added to the resin (Figure 5). The data obtained for epoxy/MWCNT composites were close to the Shore D hardness of epoxy composite based on multi-wall carbon nanotubes which were subjected to thermoelectret treatment [48]. For example, epoxy composites based on heat-treated MWCNTs showed a hardness ranging from 74–77 (Shore D). Thermoelectret treatment induced expansion of the range of hardness to 76–82.

**Figure 5.** Optical micrographs of E/0.5MWCNT (a) and E/0.5EG (b) samples (the unit scale is 200 μm).

3.4. Flammability Test

The evaluation of the flammability of the polymer materials was carried out using indicators such as the ignition temperature and the time-to-ignition. The ignition temperature is the lowest temperature at which a combustible substance, when heated, catches fire in the air and continues to burn. The time-to-ignition is defined as the minimum exposure time required for the sample to ignite and sustain a flaming combustion. The results of the experimental determination of the ignition temperature and the average time-to-ignition for the studied epoxy composites are shown in Table 4.

According to the obtained results, for the samples of epoxy composites filled with MWCNTs, a sharp growth of ignition temperature was observed from 308 °C for the pure epoxy resin E0 to 328 °C for the epoxy composite filled with 0.05 wt.% MWCNTs. With a further increase in the content of MWCNTs to 0.5 wt.%, there was a rapid decrease in the value of ignition temperature to 316 °C at 0.1 wt.%, followed by a slow decrease in the ignition temperature to 315 °C and stabilization at the content of MWCNT at 0.5 wt.%.

Table 4. Ignition temperature and time-to-ignition.

Sample	Ignition Temperature (°C)	Time-to-Ignition (s)
E0	308	437
E/0.01MWCNT	318	346
E/0.05MWCNT	328	356
E/0.1MWCNT	316	381
E/0.5MWCNT	315	446
E/0.5EG	319	371
E/1.0EG	325	334
E/1.5EG	326	367
E/2.0EG	326	348
E/2.5EG	321	346

The data on ignition temperature are in agreement with data on the kinetics of the process. For example, model-free analysis of TG data by ASTM E698 showed the activation energy of the process was 91.4 ± 16.76 kJ/mol and pre-exponential factor $\log(A/s^{-1}) = 4.6$. The activation energy slightly grows for E/0.5MWCNT compared to pure epoxy and it was 97.28 ± 15.5 kJ/mol ($\log(A/s^{-1}) = 5.11$), whereas the activation energy increases significantly for composite based on EG, and for E/0.5EG, it was 124.44 ± 7.37 kJ/mol ($\log(A/s^{-1}) = 7.56$). The results on data treatment by model-free analysis are presented in the Supplementary Materials (Figures S3–S5).

The incorporation of expanded graphite in epoxy resin also led to an increase in the ignition temperature. In this case, the rise in the ignition temperature from 308 °C for the unfilled epoxy resin E0 to 326 °C for the epoxy composite filled with 1.5 wt.% EG was observed. The further increase in the content of the EG in the epoxy resin to 2.5 wt.% caused the decrease in the ignition temperature to 321 °C.

Among the studied fillers, the maximum ignition temperature was observed for the epoxy composite filled with 0.05 wt.% MWCNTs. For the epoxy/EG composites, an increase in the ignition temperature was observed at concentrations of EG in the range of 1.0–2.5 wt.%. The char layer formed by carbon-based fillers on the surface of the epoxy matrix acts as a heat barrier [15,49] and increases the ignition temperature of the epoxy composites. At the same time, for almost all samples, a decrease in the time-to-ignition was observed compared to the pure epoxy resin, except for the sample E/0.5MWCNT. This effect is caused by the high thermal conductivity properties of MWCNTs and EG [46,50], and the increase of the epoxy composites thermal conductivity as a result of the MWCNT addition. Therefore, the ignition temperature for the epoxy/MWCNTs and epoxy/EG composites was reached faster than for the pure epoxy resin. The improvement of thermal conductivity and flammability of polypropylene composites with expanded graphite was also reported in [51]. The authors mentioned that EG did not change the mechanism of thermal degradation but retarded the evolution of volatile organic compounds during degradation. According to the shape of the TG/DSC curves, it can be concluded that our EG and MWCNT samples also did not change the mechanism of thermal oxidative degradation but played an active role in the absorption of gaseous substances formed during heating. It can be assumed that the MWCNTs had the higher volume fraction in the epoxy matrix since their aggregates are smaller than that EG, and this fact explains the higher time-to-ignition of the E/0.5MWCNT sample.

4. Conclusions

In this research, epoxy composites filled with multi-walled carbon nanotubes and expanded graphite with different loadings were prepared. The thermal oxidative degradation of the prepared samples at heating in an oxidizing environment was analyzed using thermogravimetric analysis. The parameters of the thermal-oxidative degradation of the filled samples were compared to those of the unfilled sample. The hardness of the samples was measured using the Shore D hardness test. The ignition temperature and time-to-ignition of the pure epoxy resin, epoxy/MWCNTs and epoxy/EG composites were determined. It was found that there was a rise in temperature corresponding to a 5%

weight loss during heating for both epoxy/MWCNT and epoxy/EG composites. The Shore D hardness of epoxy/MWCNTs composites increased with the content of up to 0.1 wt.% and decreased with further concentration growth. The addition of MWCNTs and EG led to an increase in the ignition temperature, but the time-to-ignition decreased, which is probably due to the growth of sample thermal conductivity. It has been shown that MWCNTs improve the thermal behavior of epoxy resin in a low-temperature region (below ~300 °C), whereas EG shows almost the same thermal behavior above 300 °C.

Supplementary Materials: The following are available online at <http://www.mdpi.com/2076-3417/10/19/6928/s1>. Figure S1: C1s XPS spectrum of EG sample. Figure S2: DSC curve of the oxidation of EG sample (air, 10 K/min, Al₂O₃). Figure S3: Results on ASTM E698 analysis of E0 sample. Figure S4: Results on ASTM E698 analysis of E/0.5MWCNT sample. Figure S5: Results on ASTM E698 analysis of E/0.5EG sample.

Author Contributions: Methodology, A.G.B.; Writing—Original draft preparation, Supervision, O.B.N.; Resources, E.A.M.; Formal analysis, M.V.P.; Investigation, I.S.B. All authors participated in the discussions of the results. All authors have read and agreed to the published version of the manuscript.

Funding: The work was funded by the State Task of Ministry of Science and Higher Education of Russia (project no. FSUN-2020-0008).

Conflicts of Interest: The authors declare no conflict of interest.

References

1. Ebewele, R.O. *Polymer Science and Technology*; CRC Press: Boca Raton, FL, USA, 2000.
2. Bower, D.I. *An Introduction to Polymer Physics*; Cambridge University Press: Cambridge, UK, 2002.
3. Lee, H.; Neville, K. *Handbook of Epoxy Resins*; McGraw-Hill: New York, NY, USA, 1967.
4. Jin, F.L.; Li, X.; Park, S.J. Synthesis and application of epoxy resins: A review. *J. Ind. Eng. Chem.* **2015**, *29*, 1–11. [[CrossRef](#)]
5. Irvine, D.J.; McCluskey, J.A.; Robinson, I.M. Fire hazards and some common polymers. *Polym. Degrad. Stab.* **2000**, *67*, 383–396. [[CrossRef](#)]
6. Vengatesan, M.R.; Varghese, A.M.; Mittal, V. Thermal Properties of Thermoset Polymers. In *Thermosets: Structure, Properties, and Applications*; Elsevier: Amsterdam, The Netherlands, 2018.
7. Wilkie, C.A.; Morgan, A.B. *Fire Retardancy of Polymeric Materials*; CRC Press: Boca Raton, FL, USA, 2010.
8. Dasari, A.; Yu, Z.Z.; Cai, G.P.; Mai, Y.W. Recent developments in the fire retardancy of polymeric materials. *Prog. Polym. Sci.* **2013**, *38*, 1357–1387. [[CrossRef](#)]
9. Shah, A.U.R.; Prabhakar, M.N.; Song, J. II Current advances in the fire retardancy of natural fiber and bio-based composites—A review. *Int. J. Precis. Eng. Manuf. Green Technol.* **2017**, *4*, 247–262. [[CrossRef](#)]
10. Schmidt, C.; Ciesielski, M.; Greiner, L.; Döring, M. Novel organophosphorus flame retardants and their synergistic application in novolac epoxy resin. *Polym. Degrad. Stab.* **2018**, *158*, 190–201. [[CrossRef](#)]
11. Guo, F.; Aryana, S.; Han, Y.; Jiao, Y. A review of the synthesis and applications of polymer-nanoclay composites. *Appl. Sci.* **2018**, *8*, 1696. [[CrossRef](#)]
12. Morgan, A.B.; Gilman, J.W. An Overview of Flame Retardancy of Polymeric Materials: Application, Technology, and Future Directions. *Fire Mater.* **2013**, *37*, 259–279. [[CrossRef](#)]
13. Gilman, J.W.; Kashiwagi, T.; Lichtenhan, J.D. A Revolutionary New Flame Retardant Approach. *SAMPE J.* **1997**, *33*, 40–46.
14. Laoutid, F.; Bonnaud, L.; Alexandre, M.; Lopez-Cuesta, J.M.; Dubois, P. New prospects in flame retardant polymer materials: From fundamentals to nanocomposites. *Mater. Sci. Eng. R Reports* **2009**, *63*, 100–125. [[CrossRef](#)]
15. Arao, Y. Flame Retardancy of Polymer Nanocomposite. In *Flame Retardants*; Springer: Cham, Switzerland, 2015; pp. 15–44. [[CrossRef](#)]
16. Nguyen, T.A.; Nguyen, Q.T.; Bach, T.P. Mechanical Properties and Flame Retardancy of Epoxy Resin/Nanoclay/Multiwalled Carbon Nanotube Nanocomposites. *J. Chem.* **2019**, 2019. [[CrossRef](#)]
17. Toldy, A.; Szebényi, G.; Molnár, K.; Tóth, L.F.; Magyar, B.; Hliva, V.; Czirány, T.; Szolnoki, B. The effect of multilevel carbon reinforcements on the fire performance, conductivity, and mechanical properties of epoxy composites. *Polymers* **2019**, *11*, 303. [[CrossRef](#)] [[PubMed](#)]
18. Zhang, Q.; Wang, Y.C.; Soutis, C.; Bailey, C.G.; Hu, Y. Fire Safety Assessment of Epoxy Composites Reinforced by Carbon Fibre and Graphene. *Appl. Compos. Mater.* **2020**, *27*, 619–639. [[CrossRef](#)]

19. Kamaraj, M.; Dodson, E.A.; Datta, S. Effect of graphene on the properties of flax fabric reinforced epoxy composites. *Adv. Compos. Mater.* **2020**, *29*. [[CrossRef](#)]
20. Wang, X.; Xing, W.; Feng, X.; Yu, B.; Song, L.; Hu, Y. Functionalization of graphene with grafted polyphosphamide for flame retardant epoxy composites: Synthesis, flammability and mechanism. *Polym. Chem.* **2014**, *5*, 1145–1154. [[CrossRef](#)]
21. Zhuo, D.; Wang, R.; Wu, L.; Guo, Y.; Ma, L.; Weng, Z.; Qi, J. Flame retardancy effects of graphene nanoplatelet/carbon nanotube hybrid membranes on carbon fiber reinforced epoxy composites. *J. Nanomater.* **2013**, *2013*, 1–7. [[CrossRef](#)]
22. Feng, Y.; He, C.; Wen, Y.; Ye, Y.; Zhou, X.; Xie, X.; Mai, Y.W. Improving thermal and flame retardant properties of epoxy resin by functionalized graphene containing phosphorous, nitrogen and silicon elements. *Compos. Part A Appl. Sci. Manuf.* **2017**, *103*, 74–83. [[CrossRef](#)]
23. Shao, Z.; Wang, H.; Li, M.; Chen, T.; Xu, Y.; Yuan, C.; Zeng, B.; Dai, L. Effect of functionalized graphene oxide with phosphaphenanthrene and isocyanurate on flammability, mechanical properties, and thermal stability of epoxy composites. *J. Appl. Polym. Sci.* **2020**, *137*, 1–11. [[CrossRef](#)]
24. Zhi, M.; Liu, Q.; Chen, H.; Chen, X.; Feng, S.; He, Y. Thermal Stability and Flame Retardancy Properties of Epoxy Resin Modified with Functionalized Graphene Oxide Containing Phosphorus and Silicon Elements. *ACS Omega* **2019**, *4*, 10975–10984. [[CrossRef](#)]
25. Mostovoy, A.S.; Yakovlev, A.V. Reinforcement of Epoxy Composites with Graphite-Graphene Structures. *Sci. Rep.* **2019**, *9*, 1–9. [[CrossRef](#)]
26. Spitalsky, Z.; Tasis, D.; Papagelis, K.; Galiotis, C. Carbon nanotube-polymer composites: Chemistry, processing, mechanical and electrical properties. *Prog. Polym. Sci.* **2010**, *35*, 357–401. [[CrossRef](#)]
27. Liew, K.M.; Lei, Z.X.; Zhang, L.W. Mechanical analysis of functionally graded carbon nanotube reinforced composites: A review. *Compos. Struct.* **2015**, *120*, 90–97. [[CrossRef](#)]
28. Bhattacharya, M. Polymer nanocomposites-A comparison between carbon nanotubes, graphene, and clay as nanofillers. *Materials* **2016**, *9*, 262. [[CrossRef](#)] [[PubMed](#)]
29. Liu, S.; Chevali, V.S.; Xu, Z.; Hui, D.; Wang, H. A Review of Extending Performance of Epoxy Resins using Carbon Materials. *Compos. Part B* **2018**, *136*, 197–213. [[CrossRef](#)]
30. Zhao, D.; Jiang, Y.; Ding, Y.; Zhu, G.; Zheng, J. Polymer/carbon nanotubes nanocomposites: Relationship between interfacial adhesion and performance of nanocomposites. *J. Mater. Sci.* **2018**, *53*, 10160–10172. [[CrossRef](#)]
31. Li, Y.; Huang, X.; Zeng, L.; Li, R.; Tian, H.; Fu, X.; Wang, Y.; Zhong, W.H. A review of the electrical and mechanical properties of carbon nanofiller-reinforced polymer composites. *J. Mater. Sci.* **2019**, *54*, 1036–1076. [[CrossRef](#)]
32. Zhang, Y.; Heo, Y.J.; Son, Y.R.; In, I.; An, K.H.; Kim, B.J.; Park, S.J. Recent advanced thermal interfacial materials: A review of conducting mechanisms and parameters of carbon materials. *Carbon N. Y.* **2019**, *142*, 445–460. [[CrossRef](#)]
33. Berdyugina, I.S.; Steksova, Y.P.; Shibaev, A.A.; Maksimovskii, E.A.; Bannov, A.G. Thermal degradation of epoxy composites based on thermally expanded graphite and multiwalled carbon nanotubes. *Russ. J. Appl. Chem.* **2016**, *89*, 1447–1453. [[CrossRef](#)]
34. Mittal, G.; Dhand, V.; Rhee, K.Y.; Park, S.-J.; Lee, W.R. A Review on Carbon Nanotubes and Graphene as Fillers in Reinforced Polymer Nanocomposites. *J. Ind. Chem. Res.* **2015**, *21*, 11–25. [[CrossRef](#)]
35. Jen, Y.M.; Huang, J.C. Synergistic effect on the thermomechanical and electrical properties of epoxy composites with the enhancement of carbon nanotubes and graphene nano platelets. *Materials* **2019**, *12*, 255. [[CrossRef](#)]
36. Kuan, C.F.; Chen, W.J.; Li, Y.L.; Chen, C.H.; Kuan, H.C.; Chiang, C.L. Flame retardance and thermal stability of carbon nanotube epoxy composite prepared from sol-gel method. *J. Phys. Chem. Solids* **2010**, *71*, 539–543. [[CrossRef](#)]
37. Gantayat, S.; Prusty, G.; Rout, D.; Swain, S.K. Expanded graphite as a filler for epoxy matrix composites to improve their thermal, mechanical and electrical properties. *Carbon N. Y.* **2016**, *98*, 734. [[CrossRef](#)]
38. Asante, J.; Modiba, F.; Mwakikunga, B. Thermal Measurements on Polymeric Epoxy-Expandable Graphite Material. *Int. J. Polym. Sci.* **2016**, *2016*, 1–12. [[CrossRef](#)]
39. Steksova, Y.P.; Berdyugina, I.S.; Shibaev, A.A.; Ukhina, A.V.; Maksimovskii, E.A.; Popov, M.V.; Bannov, A.G. Effect of synthesis parameters on characteristics of expanded graphite. *Russ. J. Appl. Chem.* **2016**, *89*, 1588–1595. [[CrossRef](#)]

40. Ferrari, A.C.; Robertson, J. Interpretation of Raman spectra of disordered and amorphous carbon. *Phys. Rev. B* **2000**, *61*, 95–107. [[CrossRef](#)]
41. Ferrari, A.C. Raman spectroscopy of graphene and graphite: Disorder, electron-phonon coupling, doping and nonadiabatic effects. *Solid State Commun.* **2007**, *143*, 47–57. [[CrossRef](#)]
42. Bannov, A.G.; Uvarov, N.F.; Ukhina, A.V.; Chukanov, I.S.; Dyukova, K.D.; Kuvshinov, G.G. Structural changes in carbon nanofibers induced by ball milling. *Carbon N. Y.* **2012**, *50*, 1090–1098. [[CrossRef](#)]
43. Nguyen, T.K.; Bannov, A.G.; Popov, M.V.; Yun, J.-W.; Nguyen, A.D.; Kim, Y.S. High-temperature-treated multiwall carbon nanotubes for hydrogen evolution reaction. *Int. J. Hydrogen Energy* **2018**, *43*, 6526–6531. [[CrossRef](#)]
44. Chairat, A.; Joulia, X.; Floquet, P.; Vergnes, H.; Ablitzer, C.; Fiquet, O.; Brothier, M. Thermal degradation kinetics of a commercial epoxy resin - Comparative analysis of parameter estimation methods. *J. Appl. Polym. Sci.* **2015**, *132*, 6–9. [[CrossRef](#)]
45. Kumar, R.; Mohanty, S.; Nayak, S.K. Study on epoxy resin-based thermal adhesive filled with hybrid expanded graphite and graphene nanoplatelet. *SN Appl. Sci.* **2019**, *1*, 1–13. [[CrossRef](#)]
46. Wang, Z.; Qi, R.; Wang, J.; Qi, S. Thermal conductivity improvement of epoxy composite filled with expanded graphite. *Ceram. Int.* **2015**, *41*, 13541–13546. [[CrossRef](#)]
47. Laachachi, A.; Burger, N.; Apaydin, K.; Sonnier, R.; Ferriol, M. Is expanded graphite acting as flame retardant in epoxy resin? *Polym. Degrad. Stab.* **2015**, *117*, 22–29. [[CrossRef](#)]
48. Bannov, A.G.; Shibaev, A.A.; Mochalova, E.N.; Galikhanov, M.F.; Limarenko, N.A.; Vakhitova, R.N. The application of carbon nanotubes for enhancement of the epoxy thermoelectret properties. In Proceedings of the 2016 11th International Forum on Strategic Technology, Novosibirsk, Russia, 1–3 June 2016.
49. Kashiwagi, T.; Mu, M.; Winey, K.; Cipriano, B.; Raghavan, S.R.; Pack, S.; Rafailovich, M.; Yang, Y.; Grulke, E.; Shields, J.; et al. Relation between the viscoelastic and flammability properties of polymer nanocomposites. *Polymer* **2008**, *49*, 4358–4368. [[CrossRef](#)]
50. Ciecierska, E.; Boczkowska, A.; Kurzydowski, K.J.; Rosca, I.D.; Van Hoa, S. The effect of carbon nanotubes on epoxy matrix nanocomposites. *J. Therm. Anal. Calorim.* **2013**, *111*, 1019–1024. [[CrossRef](#)]
51. Mochane, M.J.; Luyt, A.S. The effect of expanded graphite on the flammability and thermal conductivity properties of phase change material based on PP/wax blends. *Polym. Bull.* **2015**, *72*, 2263–2283. [[CrossRef](#)]



© 2020 by the authors. Licensee MDPI, Basel, Switzerland. This article is an open access article distributed under the terms and conditions of the Creative Commons Attribution (CC BY) license (<http://creativecommons.org/licenses/by/4.0/>).